

## Implications of varying communication speeds in “globally” coupled maps

Sudeshna Sinha

*The Institute of Mathematical Sciences, CIT Campus, Madras 600 113, India*

(Received 2 July 1997)

We have constructed a generalization of “globally” coupled maps, where the speed of information propagation can vary, giving rise to an “effective mean field,” which involves suitably time-delayed state variables of the various lattice sites. We report the wealth of spatiotemporal phases our prototypical model yields and describe the systematic effects of the various parameters on the dynamical characteristics of the system. [S1063-651X(98)03004-9]

PACS number(s): 05.45.+b, 05.50.+q

### INTRODUCTION

The coupled map lattice (CML) was introduced by Kaneko [1] as a simple model capturing the essential features of spatiotemporal dynamics in extended nonlinear systems. Over the past decade research centered around CMLs has yielded suggestive conceptual models of complex phenomena in fields ranging from biology to engineering [1]. A CML is a dynamical system with discrete time, discrete space, and continuous state variables. It usually consists of dynamical elements on a lattice that interact with suitably chosen sets of other elements. In particular, globally coupled maps (GCMs), where the coupling includes all lattice sites, has yielded a host of very different features. This class of systems is of considerable interest in modeling phenomena as diverse as Josephson junction arrays, multimode lasers, vortex dynamics, and even biological information processing, neurodynamics, and evolutionary biology. The ubiquity of distributed systems with high interconnectivity has made GCMs the focus of sustained research interest [2].

Here we propose a generalization of globally coupled maps to include a scenario where the speeds of information propagation can vary, i.e., a situation that goes beyond the usual instantaneous information exchange. This takes into account the possibility that a wide range of communication speeds may occur in a network of coupled dynamical systems. Now such a generalization of the GCM would serve as fertile ground for testing the implications of varying rates of information flow in extended systems. Further, it yields a prototypical model that can potentially be “tailored” to a wider range of phenomena, as it considers physical situations beyond the scope of current models. Some areas of immediate relevance, for instance, are neuromorphology (neurons process information from several different neurons at increasing distances, in a delayed fashion, as nonsynchronous coupling is a characteristic of chemical synapses; for instance, in the long coordinating neurons, involving long-distance coupling, the long-ranged interactions are through phase delays or lags that are determined by their distance, and these are important in understanding the complex timing relationships in intersegmental coordination [3]), optics (delays arise very naturally and ubiquitously in laser nonlinear dynamics; for instance, recent experiments on a fiber ring laser have brought to light how crucial it is to take into account delays in the coupling [4]), and electrical circuits

such as Josephson junction arrays (here too coupling via delayed fields is in fact most appropriate [5]). One can then expect that the study of retarded long-range coupling, even in toy models, would help us understand such systems better.

### I. MODEL

Now we describe the proposed class of generalized GCMs. The space on which the dynamics occurs is a discrete one-dimensional lattice, with periodic boundary conditions, where the sites are denoted by a set of integers  $i$ ,  $i = 1, \dots, N$ ,  $N$  being the linear size of the lattice. (Generalizations to higher-dimensional lattices are straightforward.) Defined on each site is a (continuous) state variable (which corresponds to the physical variable of interest) denoted by  $x_n(i)$ , where  $n$  is the discrete time. Now the local on-site dynamics is given by a suitable nonlinear map  $f(x)$ . We choose this to be the logistic map as it has widespread relevance in the context of low-dimensional chaos:  $f(x) = 1 - ax^2$ . The nonlinearity parameter  $a$  is chosen to be 2, i.e., the local dynamics is completely chaotic.

The coupling is “global” in the sense that the dynamics of a certain site is influenced by all the other sites. The crucial difference from conventional globally coupled systems is that the information of the state of the other sites is not reached instantaneously. Instead, the communication speeds are finite and local dynamical information takes a finite time to propagate through the lattice. This implies that the global coupling is incorporated through an “effective mean field” that consists of *suitably time-delayed states of the other sites*. (Such a scenario is relevant, for instance, in the context of global coupling as a simplifying mean-field-type approach to local couplings, which are usually diffusive. In such a situation, local dynamical information generically takes a finite time to travel through the lattice from the source and it is of interest to incorporate this feature in the model.)

We now define a few important parameters. First, there is the speed of information flow  $S$ . In our discrete space-time lattice this implies that information propagates to  $S$  sites (isotropically) in a single dynamical step. That is, information reaches a distance spanning  $L$  sites, after a time delay  $D = \text{int}(L/S)$  iterations. So the maximum time delay in a one-dimensional lattice of size  $N$ , with periodic boundary conditions, is  $D_{max} = \text{int}(N/2S)$ .

Then the complete dynamical picture is

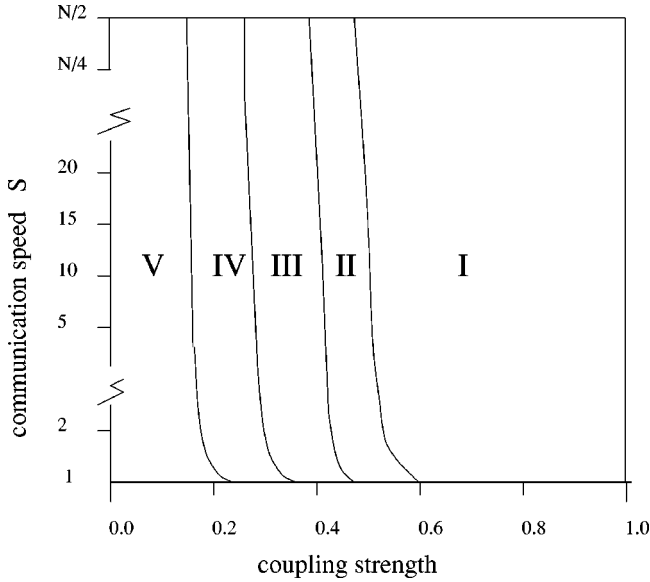


FIG. 1. Schematic phase diagram, displaying the various dynamical phases in the space of parameters: coupling strength  $\epsilon$  and communication speed  $S$  (with system size  $N=1000$ ). The phases are I, the spatiotemporal fixed point; II, the cyclic temporal evolution and oscillatory space profile; III, the cyclic temporal evolution with an irregular spatial profile; IV, noisy cycles and spatial irregularity; and V, the “turbulent” phase. See the text for a detailed description of the phases.

$$x_{n+1}(i) = (1 - \epsilon)f(x_n(i)) + \epsilon h_n(i), \quad (1)$$

where the coupling strength is given by parameter  $\epsilon$  and the effective mean field  $h_n(i)$  is given by

$$h_n(i) = \frac{1}{N} \sum_{D=0}^{D_{max}} \sum_{\Delta=S D}^{S(D+1)-1} x_{n-D}(i \pm \Delta). \quad (2)$$

(The site indices are cyclic due to periodic boundary conditions and  $\Delta \leq N/2$ .) The usual GCM limit is obtained when  $S > \text{int}(N/2)$ , which implies that the maximum delay involved is 0, i.e.,  $h_n = \sum_i x_n(i)$  [6].

## II. RESULTS

We choose random initial conditions  $x_0(i) \in [-1, 1]$  and evolve the system according to Eq. (1). After transience, we follow the dynamical evolution of the effective mean field  $h_n(i)$  and the individual state variables  $x_n(i)$  at various sites  $i$ . Note that the spectral characteristics of  $x_n(i)$  and  $h_n(i)$  are independent of the site  $i$ . (Thus we may, with no ambiguity, drop the label  $i$  in describing the time evolution of the variables  $x$  and  $h$  [7].)

### A. Dynamical phases in the model

The principal dynamical phases that emerge in the space of the two crucial parameters coupling strength  $\epsilon$  and speed of information propagation  $S$ , are the following (see Fig. 1).

(i) First is the spatiotemporal fixed point where the entire lattice is synchronized, i.e., spatially homogeneous, and each element is temporally invariant as well. This phase of the model has immediate relevance to the important and open problem of

“controlling” extended chaotic systems (which is essentially a search for algorithms that yield stable synchronized states [8]). So the emergence of synchronized fixed point dynamics from global coupling of chaotic elements may have practical utility in the control of large interactive systems.

Here we briefly assess the static and dynamic features of the solutions in this phase of the model. The static solution must satisfy the condition  $x^* = (1 - \epsilon)f(x^*) + \epsilon x^*$ , so when  $f(x) = 1 - 2x^2$ , the fixed point solutions for  $0 \leq \epsilon < 1$  are  $x^* = 1/2$  and  $-1$ . Linear stability of the static solution yields (taking into account the fact that  $x_{n-D} = x^*$  for  $D > 0$  and  $x_{n-D} = x^* + \delta x$  for  $D = 0$ ) the  $N \times N$  stability matrix  $J = (1 - \epsilon)f'(x^*)I + (\epsilon/N)M$ , where the matrix  $I$  is an identity matrix and the matrix  $M$  has entries  $M(i, j) = 1$  when  $|j - i| \leq S$ , with  $i, j$  arranged cyclically. The magnitude of the eigenvalues of  $J$  [ $\Lambda_j = (1 - \epsilon)f'(x^*) + (\epsilon/N)\lambda_j$ , where  $\lambda_j, j = 1, \dots, N$ , are the eigenvalues of the matrix  $M$ ] will indicate the stability of the spatiotemporal fixed point  $x^*$ . For example, for  $S \sim N/2$  it is easily seen that this gives the stable range of  $\epsilon$ , for  $x^* = 0.5$ , to be  $\epsilon > \frac{1}{2}$ , which agrees completely with the values obtained numerically.

(ii) The evolution is a cycle temporally, with a traveling-wave-like oscillatory space profile. An interesting feature of these spatial undulations is the dependence of the period of spatial oscillations  $T_{space}$  on the maximum delay in the effective mean field, namely,

$$T_{space} = D_{max} + 1$$

(see Fig. 2). Thus the dynamics in this phase present an alternate way of producing traveling-wave solutions in spatially extended systems (and this may be quite relevant in the neuronal context of intersegmental coordination, such as that responsible for undulatory locomotion [3]).

(iii) The evolution is a cycle temporally, with an irregular spatial profile.

(iv) The system evolves as noisy cycles and is irregular spatially. Spectra of dynamical quantities such as  $h$  and  $x$  in this phase are characterized by prominent  $\delta$  spikes on a noisy broad background and are very similar to the spectra associated with “periodic chaos” [9].

(v) The system displays no apparent regularity or correlations in time or space. We call this phase “turbulent” [10]. Later we will describe the surprising emergent features of the effective mean field in this phase.

In Fig. 3 we display bifurcation diagrams indicating the details of the phases, as reflected in the value of the effective mean field, for varying values of coupling strengths  $\epsilon$ , at different communication speeds  $S$ . These diagrams represent four horizontal cuts, at  $S = 1, 25, 125, 250$ , in Fig. 1.

### B. Transient dynamics

In recent years, rather exciting features of transience, closely related to many aspects of nonlinear dynamics, are being brought to light in both numerical and laboratory experiments [11]. These developments have motivated us here to research in depth the transient phenomena emerging from our model. The spectral characteristics of transient dynamics can be constructed by taking transient time series of independent runs of reasonable length and averaging their power spectra. We found that the power spectrum of the effective

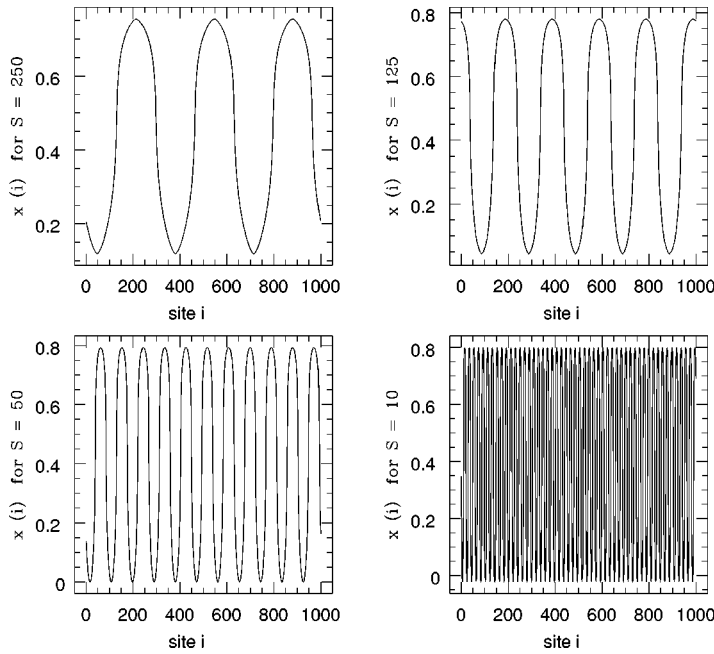


FIG. 2. Spatial profile  $x(i)$  vs  $i$  for a system of size  $N=1000$ , at  $\epsilon=0.5$  and communication speed  $S=250, 125, 50$ , and  $10$ .

mean field (computed in this manner) displayed clear  $1/f^2$  behavior in the  $\epsilon < 0.5$  phase (see Fig. 4). As the system size  $N$  was increased and communication speed  $S$  decreased, the transience grew as  $\sim N/2S$ . The evolution of individual sites did not show any evidence of this long transient behavior and was merely noisy and flat [12]. This emergence of dynamically significant global transient phenomena from short featureless local transience can provide a fertile ground for future numerical and experimental investigations.

One can rationalize this interesting transient phenomenon as follows: When  $\epsilon$  is low, the dynamics of the state variables at each site  $x(i)$  is chaotic and so the transient process and the evolution thereafter behaves almost like quasirandom numbers, thus yielding white-noise-like flat power spectra  $P(f) \sim 1/f^0$  [13]. On the other hand, when the information

propagation speed  $S$  is finite, collective quantities such as the effective mean field will have a transient process quite like a “random-walk” function, i.e., from some initial value the effective mean field will evolve essentially as a running sum, incrementing  $2S$  “random” components at each dynamical time step. After  $n = N/2S$  iterations then, it will arrive at the first “bonafide” effective mean field, i.e., a mean field that is comprised entirely of state variables evolving under their asymptotic dynamics. This marks the end of the transient process. So the transience time is  $N/2S$  (which tends to infinity for low  $S$  as the system size  $N \rightarrow \infty$ ) and is an integrated white-noise process, which naturally leads to  $P(f)$

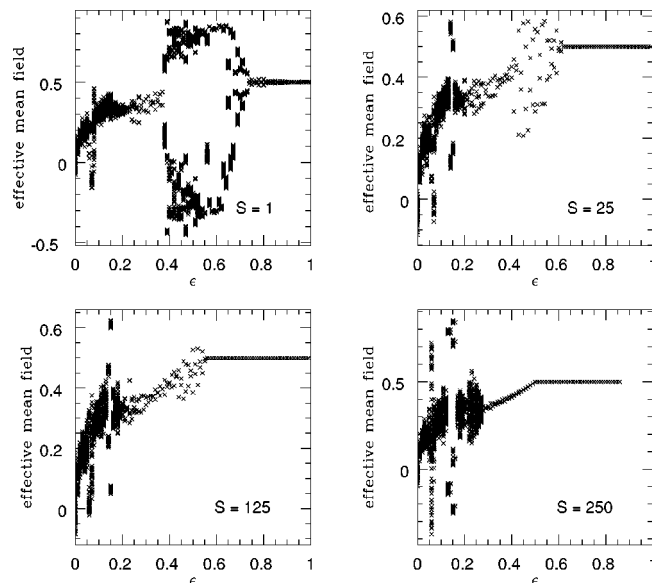


FIG. 3. Bifurcation diagrams showing the effective mean field vs coupling strength  $\epsilon$ , for four values of communication speeds:  $S=1, 25, 125$ , and  $250$ .

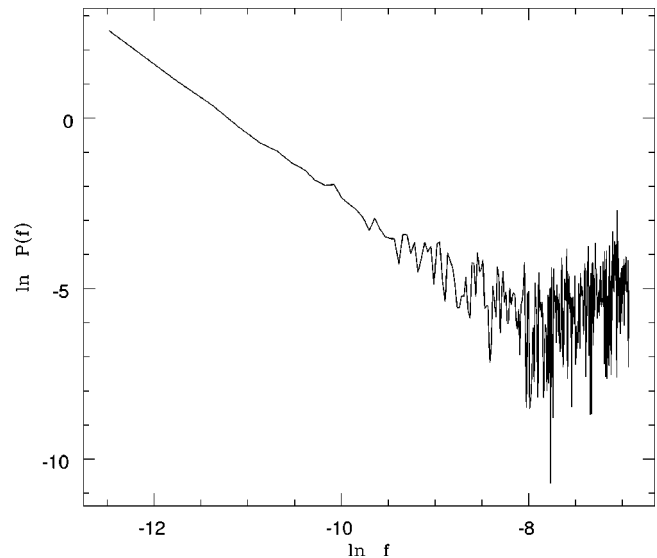


FIG. 4. Power spectrum of the transient dynamics of the effective mean field in a system with  $S=1$ ,  $\epsilon=0.1$ , and  $N=1000$ . Here we average over 20 transient runs of length 512 each. On the abscissa we have  $\ln f$ , where  $f$  is the frequency, and on the ordinate we have  $\ln P(f)$ , where  $P$  is the power. [See Fig. 5(b) for the power spectrum of the asymptotic dynamics of the effective mean field for a comparison with the transient dynamics given here.]

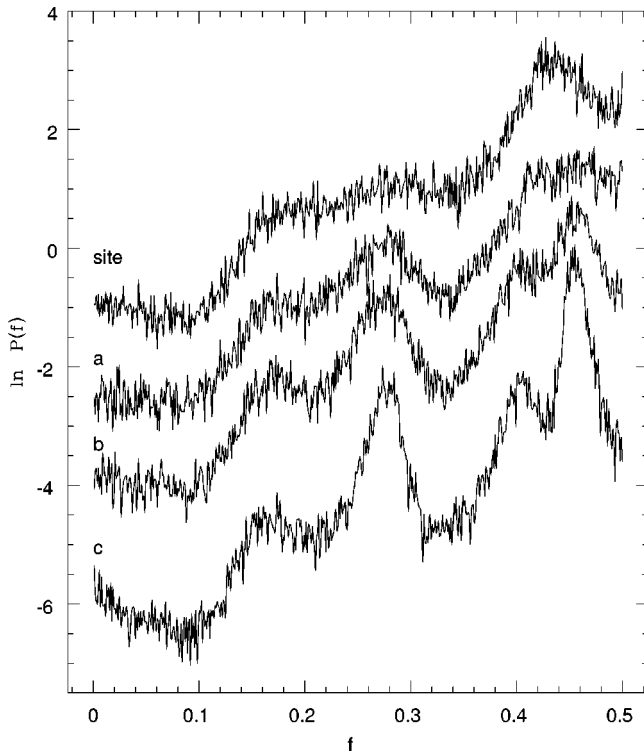


FIG. 5. Power spectra of the effective mean field when  $S=1$ ,  $\epsilon=0.1$ , and system size  $N=250$ ,  $1000$ , and  $4000$  for curves  $a$ ,  $b$ , and  $c$ , respectively. The power spectrum of a single site in a lattice of size  $N=1000$  is also shown above the mean-field spectra. Here we average over 20 runs of length 1024 each. On the ordinate we have  $\ln P(f)$ , where  $P$  is the power, and on the abscissa we have  $f$ , which is the frequency. Note that we have taken care to discard the long transience mentioned in the text. [The units of the ordinate  $\ln P(f)$  have been translated for two spectra by additive constants for ease of visualization. Curve  $c$  is shifted down by 1 and the spectrum of the single site by 4.]

$\sim 1/f^2$  [14]. This is exactly what is observed numerically in extensive simulations: The transient times scale as  $N/2S$  and the transient spectra display power  $P(f) \sim 1/f^2$ . So low information propagation speeds can yield an arbitrarily long transient dynamics for collective quantities, with well-defined  $1/f^2$  spectral characteristics. It thus constitutes another mechanism for (or, alternately, can be considered another source of) generating low-frequency noise in large systems.

### C. Emergent coherence in the turbulent phase

It was observed, in previous studies of the “turbulent” phase of GCMs ( $S \sim N/2$ ), that while there was no explicit evidence of correlation among the elements, there were pronounced signatures of subtle collective behavior [2]. This was manifested in the development of broad peaks in the power spectra of collective quantities, such as the mean field, as the number of elements coupled was increased (though the individual evolutions were chaotic). Now it is valuable to ascertain which of these emergent features of conventional GCMs persist at finite communication speeds (i.e., when  $S < N/2$ ), especially in view of the fact that the implicit time averaging involved in constructing an effective mean field from delayed variables may be expected to eliminate the collective coherence [15].

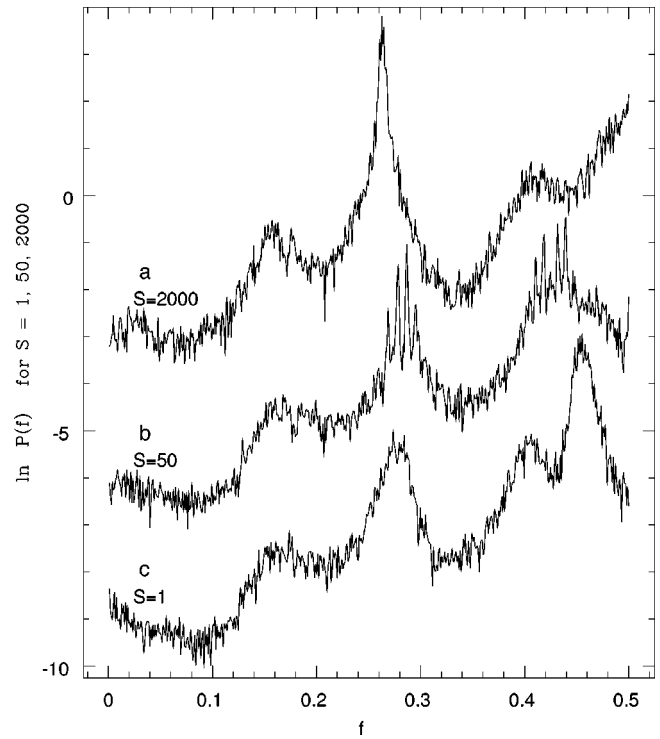


FIG. 6. Power spectra of the effective mean field when  $N=4000$ ,  $\epsilon=0.1$ , and communication speed  $S=2000$ ,  $50$ , and  $1$  for curves  $a$ ,  $b$ , and  $c$ , respectively. Here we average over 20 runs of length 1024 each. On the ordinate we have  $\ln P(f)$ , where  $P$  is the power, and on the abscissa we have  $f$ , which is the frequency. [The units of the ordinate  $\ln P(f)$  have been translated for two spectra by additive constants for ease of visualization. Curve  $b$  is shifted down by 1 and curve  $c$  by 4.]

However, interestingly, one observes the development of global “beating” patterns in our effective mean field, as manifest in the emergence of peaks (of varying degrees of sharpness) in the spectra for all values of communication speeds  $S$ . This is very evident in the example displayed in Fig. 5, where we have the slowest possible communication speed, namely,  $S=1$ , which is very far indeed from  $S \sim N/2$  corresponding to the usual GCM. Here too it is clear that prominent broad peaks begin to emerge in the spectra of the effective mean field, as lattice size increases, indicating the development of collective “modes” in the global dynamics of large systems. Note the contrast with the spectra of a single site (given in the same figure for reference), which is always noisy and flat (even in very large lattices), reflecting the chaotic evolutions of the individual sites. It is quite remarkable, then, that the *sequence of past states of the sites develop certain sustained correlations, which result in the development of rough quasiperiodicities in the effective mean field*. These “memory” effects in the dynamics, which allow the site variables to conspire over a span of  $D_{max}$  iterations to produce a regularly beating mean field, are amazing, especially if one takes note of the fact that each individual site is losing track of its previous state exponentially fast due to the existence of positive Lyapunov exponents [16].

The magnitude of the spectral peaks expectedly [15] decrease as  $S$  decreases from the globally coupled limit, i.e., when  $S < N/2$ . However, remarkably, we find that as  $S$  is

lowered much further, i.e., pushed towards the other extreme limit  $S \rightarrow 1$ , the peaks begin to become pronounced again. For instance, in the examples shown in Fig. 6 (lattice size  $N=4000$ ) the peak is very prominent for  $S=2000$ . Then, as  $S$  is lowered it becomes more broad and rough (like at  $S=50$ , which is displayed), but as  $S$  is decreased further the peaks in the spectra become more pronounced again (the limiting case of  $S=1$  is shown) [17].

### CONCLUSION

In summary, we have constructed a generalized GCM incorporating the provision of varying communication speeds. A variety of dynamical phases emerge, depending on the rate of information propagation  $S$  ( $1 \leq S \sim N/2$ ) and strength of coupling  $\epsilon$ . The emergent phenomena include spatiotemporal fixed points and spatiotemporal cycles, marked by  $S$  dependent traveling-wave-like spatial oscillations. We have also

brought to light some different transient dynamics of the effective mean field, which displays very clear  $1/f^2$  spectral characteristics, with the length of transience scaling as  $N/2S$ . Further, in the turbulent phase of our system, one observed the emergence of certain persisting subtle coherences, as reflected in the development of prominent peaks in the spectra of the effective mean field, for all values of communication speeds  $S$ . These effects were most enhanced in the limit of very large  $S$ , followed by weak effects at moderate  $S$  and remarkably enough (defying expectations of time averaging blurring these effects) rather more pronounced collective modes again at very small  $S$ .

### ACKNOWLEDGMENT

I would like to thank Gabriel Perez for many stimulating discussions on this topic.

- 
- [1] *Theory and Applications of Coupled Map Lattices*, edited by K. Kaneko (Wiley, New York, 1993), and references therein; J. Crutchfield and K. Kaneko, in *Directions in Chaos*, edited by Hao Bai-Lin (World Scientific, Singapore, 1987), and references therein.
- [2] K. Kaneko, Phys. Rev. Lett. **63**, 219 (1989); Physica D **41**, 38 (1990); Phys. Rev. Lett. **65**, 1391 (1990); Physica D **55**, 368 (1992); **54**, 5 (1991); G. Perez *et al.*, Phys. Rev. A **45**, 5469 (1992); Physica D **63**, 341 (1993); G. Perez and H. A. Cerdeira, Phys. Rev. A **46**, 7492 (1992); S. Sinha *et al.*, *ibid.* **46**, 3193 (1992); **46**, 6242 (1992); D. Dominguez and H. A. Cerdeira, Phys. Rev. Lett. **71**, 3359 (1993).
- [3] A. H. Cohen and T. Kiemal, Am. Zool. **33**, 54 (1993).
- [4] Q. L. Williams and R. Roy, Opt. Lett. **21**, 1478 (1996); Q. L. Williams, T. Garcia-Ojalvo, and R. Roy, Phys. Rev. A **55**, 2376 (1997).
- [5] K. Weisenfeld (private communication).
- [6] There is scope and relevance for introducing a more general definition of the ‘‘effective mean field’’ where the influence of the delayed states is weighted by some function of the delay.
- [7] Note that in our study we have updated the sites in a certain fixed order (say, starting from lattice site  $i=1$ , going on to  $i=N$ ) and at each step we use the *current* values of  $x(i)$  to compute the effective mean field via Eq. (2). On the other hand, if one computed the effective mean field synchronously at the beginning of each time step and updated each site simultaneously, the resulting numbers could sometimes be a little different, but the emergent qualitative picture would be identical. So the results quoted here hold, regardless of the updating algorithm.
- [8] Some references of this rapidly growing field of interest are L. Pecora and T. L. Carroll, Phys. Rev. Lett. **64**, 821 (1990); Phys. Rev. A **44**, 2374 (1991); T. L. Carroll, Phys. Rev. E **50**, 2580 (1994); J. F. Heagy, T. L. Carroll, and L. M. Pecora, *ibid.* **50**, 1874 (1994); D. Auerbach, Phys. Rev. Lett. **72**, 1184 (1994).
- [9] S. Thomae and S. Grossmann, J. Stat. Phys. **26**, 485 (1981).
- [10] The word ‘‘turbulent’’ is used in the same sense as it has been earlier used in the context of conventional GCM [2].
- [11] T. Tel, in *Directions in Chaos*, edited by Hao Bai-Lin (World Scientific, Singapore, 1990), Vol. 3, p. 149; I. Janosi and T. Tel, Phys. Rev. E **49**, 2756 (1994); K. G. Szabo and T. Tel, Phys. Lett. A **196**, 173 (1994); I. Janosi, L. Flepp, and T. Tel, Phys. Rev. Lett. **73**, 529 (1994); S. Sinha, Phys. Rev. E **53**, 4509 (1996).
- [12] One should also note that the above transient behavior is different from the long transience at around  $\epsilon=0.5$ , which marks the transition to a spatiotemporally coherent phase. Unlike our situation, the phenomena at  $\epsilon \sim 0.5$  is akin to the long transience present at bifurcation points due to marginal stability and is characterized by low-frequency noise in the power spectra of *both* the individual elements and the mean field.
- [13] See Fig. 5 for an example of a single site spectrum (which is the topmost curve).
- [14] W. H. Press, Comments. Astrophys. **7**, 103 (1978).
- [15] A. Pikovsky, Phys. Rev. Lett. **71**, 653 (1993).
- [16] The observations in this paper complement a recent study on GCM [G. Perez, S. Sinha, and H. A. Cerdeira, Phys. Rev. E **54**, 6936 (1996)] where mean fields were either delayed by a certain amount  $D$  or averaged over  $P$  contiguous iterations. Our scenario, however, is not equivalent to either delayed or averaged mean field, but involves a bit of both. On the one hand, it has a summation over sites at different time steps (akin to averaging) and, on the other hand, it also has a sum over a subset of sites delayed by a certain amount (akin to a delayed mean field). Analyzing the magnitude of influence of these two competing trends (with respect to increasing  $D$  and  $P$  on varying subsets of the lattice) may shed some light on the underlying phenomena.
- [17] Note here that there are two prominent frequencies in the system, given by the most pronounced peak at  $S \rightarrow N/2$  and at  $S \rightarrow 1$  (see Fig. 6). At intermediate  $S$  lying in between these two limits, we observe less pronounced peaks [often with finer frequencies resolved around the broadest peak(s)] at roughly these two positions (as is evident from the case of  $S=50$  in Fig. 6).